The EPR Spectra of Thiyl Radical Spin Adducts Produced by Photolysis of Disulfides in the Presence of 2,4,6-Tri-*tert*-butylnitrosobenzene and 5,5-Dimethyl-1-pyrroline *N*-Oxide

Brynmor Mile,[a] Christopher C. Rowlands,[a] Philip D. Sillman[a] and Melanie Fildes[b]
[a] *School of Chemistry and Applied Chemistry, University of Wales College of Cardiff, P.O. Box 912, Cardiff CF1 3TB, UK*
[b] *Shell Research Limited, Thornton Research Centre, P.O. Box 1, Chester CH1 3SH, UK*

A series of thiyl radicals prepared by the photolysis of the parent disulfide have been trapped using 5,5-dimethyl-1-pyrroline *N*-oxide (DMPO) and 2,4,6-tri-*tert*-butylnitrosobenzene (BNB). The EPR spectra of the resulting spin adducts show proton hyperfine interactions from the δ-protons of the alkyl group of the thiyl, thus allowing definitive radical assignments to be made. For thiyl BNB spin adducts, a characteristic nitrogen coupling constant is observed. For secondary and tertiary thiyls, two adducts arise from addition to the nitrogen and oxygen of the nitroso group. The extent of reaction at the oxygen increases with increasing disulfide concentration. This is attributed to the formation of a complex between the thiyl and the parent disulfide, whose bulk favours its addition to the less sterically hindered oxygen position. The rate constant for the reaction of $Pr^iS^{\bullet}$ radicals with $(Pr^iS)_2$ to form the complex is 240 times lower than that for reaction with BNB. Direct addition of $Pr^iS^{\bullet}$ to the nitrogen of BNB is 11.5 times more efficient than to oxygen.

Thiyl radicals are intermediates in biological systems[1] and in the reactions of sulfur-containing antioxidants in hydrocarbon oxidation.[2] Unfortunately, these radicals cannot be detected directly in solution by EPR spectroscopy owing to their large *g*-factor anisotropy. This anisotropy arises from the near degeneracy of the two π-type orbitals at the sulfur centre which causes such extensive line broadening as to make the radicals unobservable in the liquid phase.[3] Thus, in order to observe thiyl radicals by EPR spectroscopy, spin traps have to be employed which convert the thiyl radicals to 'stable' spin adducts which can be readily detected.[4]

In this study, thiyl radicals were produced by the photolysis of the corresponding disulfides, RSSR, which results in homolytic scission of the S–S bond.[5,6,7] The thiyl radicals produced were then trapped using either 5,5-dimethyl-1-pyrroline *N*-oxide (DMPO) or 2,4,6-tri-*tert*-butylnitrosobenzene (BNB).

DMPO, a cyclic nitrone, has only one possible trapping site (Scheme 1) so that no relative steric effects are discernible. It has also been shown to be an efficient trap for thiyl radicals[7,9] and, interestingly, hyperfine interactions with protons other than the unique β-proton have been reported.[4,9] However, from these studies it was not possible to decide whether these additional proton interactions arose from δ-protons of the thiyl groups or from γ-protons on the ring of the DMPO itself. Additional proton interactions in other DMPO spin adducts with heteroatoms, such as nitrogen and oxygen, bonded at the C-2 position have been assigned to γ-protons at the C-3 and C-4 ring positions and taken to indicate non-polarity at the nitroxyl function.[10] A firm assignment can be made by selective deuteriation of the reactants or by studying a series of thiyls with different numbers of δ-protons, which is the approach we have taken here.

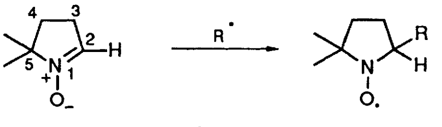

Scheme 1

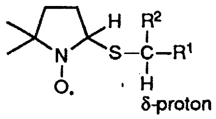

BNB was first used as a spin trap by Terabe and Konaka,[8] who found that it had two trapping sites, the nitrogen and oxygen atoms of the nitroso group (Scheme 2). The *N*-alkoxyanilino radicals (**1b**) are distinguishable from the nitroxides (**1a**) by their different *g*-values and the values of the nitrogen and *meta*-proton hyperfine coupling constants. Addition of radicals to BNB is sterically dependent. *N*-Alkoxyanilino radicals (**1b**) are less stable than the nitroxide radical (**1a**) so that, energetically, addition to the nitrogen atom is preferred. However, the addition of sterically bulky radicals to nitrogen is disfavoured by the presence of large *tert*-butyl groups at the *ortho* positions of the phenyl ring. Terabe and Konaka found that primary alkyl radicals added exclusively to nitrogen, secondary alkyl radicals to both nitrogen and oxygen and tertiary alkyl radicals added exclusively to oxygen. The only previously reported thiyl radical trapped by BNB was $PhS^{\bullet}$[7] which had a very distinctive nitrogen hyperfine coupling.

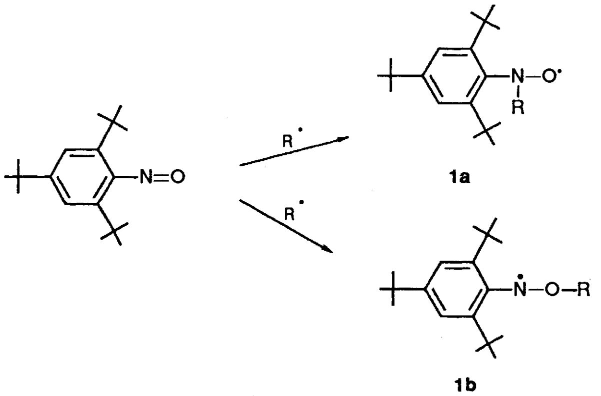

1a

1b

Scheme 2

Table 1 Hyperfine interactions in DMPO spin adducts of thiyl radicals in toluene[a]

Thiyl	a_N/mT	$a_{\beta\text{-H}}$/mT	$a_{\delta\text{-H}}$/mT	T/K
CH_3S	1.32 (1.533)[b]	1.07 (1.80)[b]	0.10 (3 H)	216
C_2H_5S	1.31 (1.533)[b] (1.34)[c]	1.03 (1.77)[b]	0.11 (2 H)	220
$C_{12}H_{25}S$	1.31	1.06	0.10 (2 H)	246
$C_{16}H_{33}S$	1.31	1.06	0.10 (2 H)	258
$PhCH_2S$	1.34 (1.36)[c]	1.12 (1.17)[c]	0.11 (2 H)	258
$(CH_3)_2CHS$	1.31 (1.35)[c]	1.03 (1.12)[c]	0.10 (1 H)	221
$(CH_3)_3CS$	1.325 (1.34)[c]	1.04 (1.12)[c]		258
PhS	1.29	1.41		223

[a] $g = 2.006 \pm 0.0005$. [b] Values in water (ref. 7). [c] Values in benzene (ref. 9).

Table 2 Hyperfine parameters for thiyl radicals trapped by BNB in toluene[a]

Thiyl	a_N/mT	$a_{m\text{-H}}$/mT	$a_{\delta\text{-H}}$/mT
CH_3S	1.56	0.09	0.17 (3 H)
C_3H_7S	1.58	0.08	0.115 (2 H)
$C_{16}H_{33}S$	1.58	0.08	0.115 (2 H)
$C_{12}H_{25}S$	1.58	0.08	0.115 (2 H)
$(CH_3)_2CHS$	1.58	0.08	0.11 (1 H)
	1.0[b]	0.19	
Bu^tS	1.6	0.08	
	1.01[b]	0.18	
PhS	—		
$PhCH_2S$	—		

[a] $g = 2.007 \pm 0.0005$. [b] $g = 2.004 \pm 0.0005$.

Experimental

All spectra were recorded on a Varian E-109 X-band spectrometer employing 100 kHz modulation. Toluene solutions of the parent disulfide and spin trap were deoxygenated using the freeze/thaw method and photolysed in the cavity of the spectrometer with unfiltered light from a Kratos 1 kW Xenon arc lamp.

For spectra recorded below ambient temperatures a modified Oxford Instruments temperature controller was used, the temperature recorded being accurate to within ±0.5 K. Temperatures were varied until the best resolved spectra were obtained.

The concentration of disulfide used ranged between 10^{-4} and 10^{-1} mol dm^{-3} for $(C_{16}H_{33}S)_2$, $(C_{12}H_{25}S)_2$, $(PhS)_2$ and $(PhCH_2S)_2$ and between 10^{-4} mol dm^{-3} and neat liquid for $[(CH_3)_2CHS]_2$, $(CH_3S)_2$, $(C_3H_7S)_2$, $(C_2H_5S)_2$ and $(Bu^tS)_2$. Spin trap concentrations were usually kept constant at 5×10^{-3} mol dm^{-3} except for $(PhS)_2$ and $(PhCH_2S)_2$ where the BNB concentration was increased to 2.5×10^{-2} mol dm^{-3}.

For the kinetic analysis of the BNB spin adducts from $(CH_3)_2CHS^{\bullet}$ the concentration of $[(CH_3)_2CHS]_2$ was varied from 2.5×10^{-3} to 1×10^{-2} mol dm^{-3} and BNB from 2.5×10^{-3} to 1×10^{-2} mol dm^{-3}. Photolysis of solutions of $[(CH_3)_2CHS]_2$ and BNB were carried out until steady states of the spin adducts were produced. The peak heights and line widths of the adducts were recorded along with their decay characteristics.

g-Values of the spin adducts were determined using DPPH as a reference. The observed spectra were simulated using our in-house isotropic simulation programme or that available with the JEOL Esprit Unit. $(C_{16}H_{33}S)_2$ and $(C_{12}H_{25}S)_2$ were kindly supplied by Shell Research Ltd. $(PhS)_2$, $(PhCH_2S)_2$, $(Bu^tS)_2$, $(CH_3S)_2$, $(CH_3CH_2S)_2$, $[(CH_3)_2CHS]_2$, $(C_3H_7S)_2$ were commercially available samples (Aldrich) with purities greater than 97% and were used without further purification. The spin traps BNB and DMPO were obtained from Aldrich.

Results and Discussion

Trapping of Thiyl Radicals with DMPO.—Photolysis of a solution of DMPO alone produced no spectrum and all thiyl spin adducts decayed rapidly after photolysis was stopped. Representative experimental and simulated spectra of the thiyl DMPO spin adducts produced by photolysis of a series of disulfides are shown in Fig. 1 and the EPR parameters derived from the spectra and optimised by computer simulation are listed in Table 1. The temperatures quoted in the table are those at which the spectra showed maximum resolution.

Only one disulfide, benzyl disulfide, gave a mixed adduct spectrum and the ratio of the two adducts did not vary with change in disulfide concentration. The second species trapped had similar nitrogen and hydrogen coupling constants to those reported for the benzyl radical,[11,12] which probably results from photocleavage of the C–S bond.

The spectra show clearly that the additional hyperfine multiplets match exactly the number of δ-protons in the thiyl R-group: singlets for $Bu^tS^{\bullet}$, $PhS^{\bullet}$; a doublet for $Pr^iS^{\bullet}$; triplets for $C_2H_5S^{\bullet}$, $C_{12}H_{25}S^{\bullet}$, $C_{16}H_{33}S^{\bullet}$ and $PhCH_2S^{\bullet}$; and a quartet for $CH_3S^{\bullet}$. This is good evidence that the additional proton interactions arise from the δ-protons of the thiyl group. It is highly unlikely that different alkyl groups in the thiyl component would change the conformation of the ring in such a way as to produce an accidental coincidence of interactions with different numbers of ring γ-protons to match exactly the pattern expected from the thiyl protons.

The optimised spectra allow the type of thiyl radical trapped, $R_3CS^{\bullet}$, $R_2CHS^{\bullet}$, $RCH_2S^{\bullet}$ or $CH_3S^{\bullet}$ to be unequivocally assigned. Unlike thiyl radicals, the corresponding adducts from alkoxy radicals have been reported to give rise to a large hyperfine interaction from one ring γ-proton at C-3 (0.206 mT and 0.23 mT for DMPO adducts of $BuO^{\bullet}$ and $Bu^tO^{\bullet}$). This has been interpreted to indicate a ring puckering at C-2.[10] No such interactions are observed for thiyl radicals indicating that no conformational changes are induced in this case. The differences between alkoxyl and thiyl radicals probably arise from: (i) the lower electronegativity of the sulfur which lowers γ-proton interactions; (ii) the availability of low-lying d orbitals on sulfur which allows delocalisation of the electron into the attached alkyl group, thus leading to significant δ-proton interactions.

There is an interesting reversal in the relative magnitudes of the nitrogen and proton hyperfine interactions in the phenyl thiyl adduct where $a_N < a_{\beta\text{-H}}$. A similar reversal has been reported for chlorophenylthiyl and triphenylmethylthiyl spin adducts of DMPO.[13] This may indicate electron withdrawal from the nitroxyl function towards the aromatic π-systems of the phenyl groups through the mediation of sulfur d orbitals.

The nitrogen and β-proton hyperfine interactions reported here are close to those found for the same adducts in benzene and lower than those in water[6] in accordance with the known increase in interaction constants with increase in relative permittivity of the solvent.[4] There is also a reversal of the nitrogen and proton hyperfine interaction in water, $a_N < a_H$ which probably arises from increased charge separation in the HOMO at the nitroxide group and a corresponding decrease in unpaired electron density at this group in the SOMO.

Trapping of Thiyl Radicals with BNB.—No spin adducts were observed on photolysing solutions of BNB. Representative experimental and simulated spectra of the BNB spin adducts from the photolysis of a series of disulfides are shown in Figs. 2 and 3. The EPR parameters derived from the spectra and optimised by computer simulation are listed in Table 2. The high field lines are broadened owing to M_I effects and incomplete averaging of the anisotropic components caused by the molecule not freely tumbling in solution. These effects are included in the simulations.

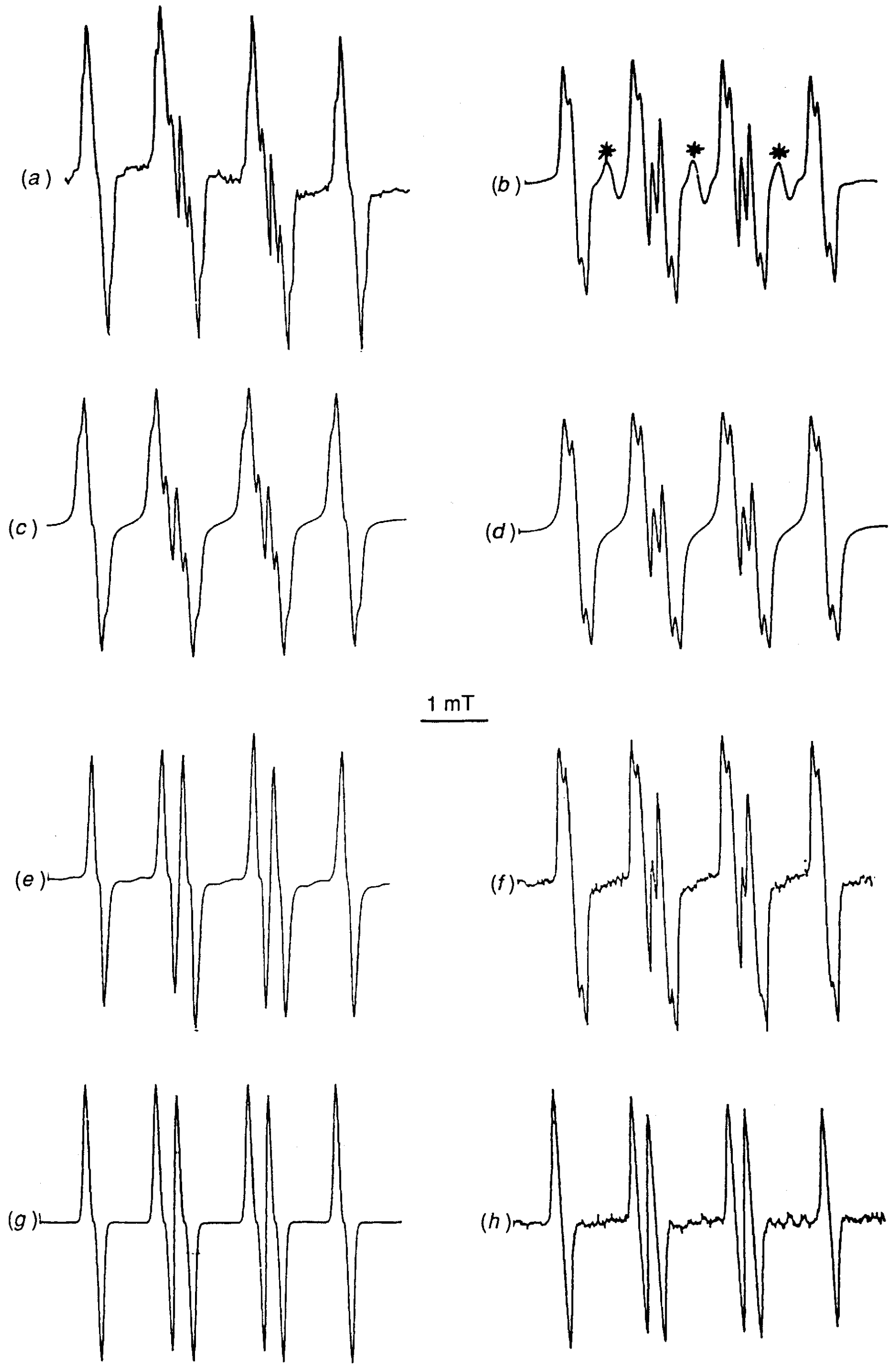

Fig. 1 Experimental and simulated EPR spectra of thiyl spin adducts of DMPO in toluene. Adducts of: (*a*) $CH_3S^\bullet$, (*b*) $C_2H_5S^\bullet$, (*e*) $Pr^iS^\bullet$, (*f*) $C_{12}H_{25}S^\bullet$, (*h*) $Bu^tS^\bullet$. (*c*), (*d*) and (*g*) are simulations of spectra (*a*), (*b*) and (*e*) using the parameters given in Table 1. * Unidentified transitions probably arising from photodecomposition of the spin trap.

Photolysis of the disulfides $(MeS)_2$, $(EtS)_2$, $(PrS)_2$ and $(C_{12}H_{25}S)_2$ and $(C_{16}H_{33}S)_2$ gave EPR spectra of the nitroxide adduct (**1a**) over the complete disulfide concentration range. No transitions from adduct **1b** arising from addition at the oxygen were detected. These spin adducts all had a characteristic large nitrogen coupling constant of *ca.* 1.6 mT. This is in agreement with Terabe and Konaka who reported $a_N = 1.63$ mT for the $PhS^\bullet$ spin adduct in benzene.[8]

In sharp contrast, photolysis of 10^{-4} mol dm^{-3} solutions of $(Bu^tS)_2$ and $(Pr^iS)_2$ gave two spin adducts from addition to both oxygen and nitrogen. The two adducts have distinctively different g values (**1a**, $g = 2.007$; **1b**, $g = 2.004$) and nitrogen and *meta*-proton interactions and are readily distinguished. Increasing the concentration of disulfide resulted in a progressive increase in the extent of addition to oxygen until, in neat disulfide, only this adduct was observed, at a spin trap concentration of 5×10^{-3} mol dm^{-3} [Fig. 3(*c*) and (*f*)]. When the spin trap concentration in pure disulfide was increased to 1×10^{-2} mol dm^{-3}, both adducts were observed.

No spin adducts were observed from phenyl or benzyl disulfide even when the disulfide concentration was increased to 10^{-1} mol dm^{-3} and BNB concentration to 2.5×10^{-2} mol dm^{-3}. This is in contrast to the results of Terabe and Konaka who reported the trapping of $PhS^\bullet$ on photolysis of $(PhS)_2$. We have no explanation for this difference.

For the nitroxide spin adducts (**1a**) hyperfine interactions with the δ-protons of the thiyl group were also observed in addition to those with the nitrogen and *meta*-ring-protons.

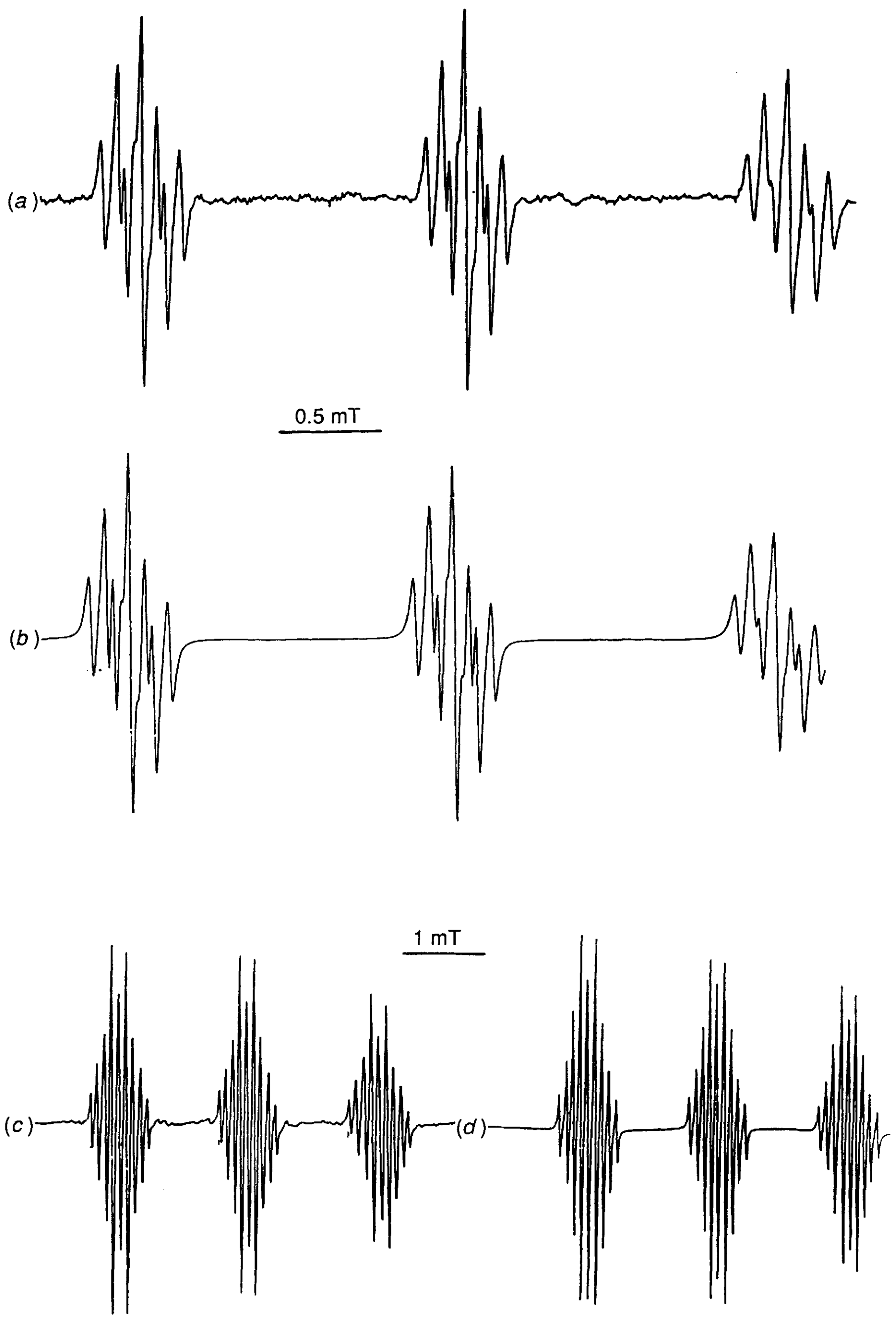

Fig. 2 Experimental and simulated EPR spectra of thiyl spin adducts of BNB in toluene. Adducts of: (*a*) $C_{16}H_{33}S^{\bullet}$, (*c*) $CH_3S^{\bullet}$. (*b*) and (*d*) are simulations of spectra (*a*) and (*c*) using the parameters given in Table 2.

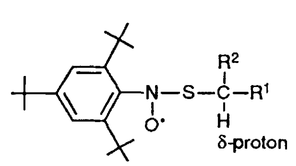

These additional hyperfine interactions are of similar magnitude to the *meta*-protons and good simulations of experimental spectra could only be achieved by inclusion of the correct number of these δ-protons, three for $CH_3S^{\bullet}$, two for $CH_3CH_2S^{\bullet}$ and one for $(CH_3)_2CHS^{\bullet}$ *etc*. This is the first definitive evidence of δ-proton hyperfine interactions in thiyl adducts of BNB.

The number of δ-protons observable in adduct spectra enables the type of alkyl group on the thiyl radical to be determined relatively easily. Thiyl spin adducts of BNB are readily distinguished from alkyl spin adducts because of their much higher nitrogen hyperfine interactions (*cf.* $Me^{\bullet}$ with a_N = 1.3 mT and $MeS^{\bullet}$ with a_N = 1.59 mT). The *meta* hydrogen coupling is approximately the same for both types of radical adduct. The increase in a_N indicates an increasing nitrogen 2s orbital contribution to the SOMO at the nitrogen centre. This probably arises because the more electronegative thiyl radical results in a slight change towards a pyramidal conformation at the nitrogen (*i.e.* increasing sp^x contributions) in comparison with alkyl addition, where the molecule retains its planar nature at nitrogen. This change will have little effect on the *meta* hydrogens and these coupling constants will be similar to those in the corresponding alkyl radical.

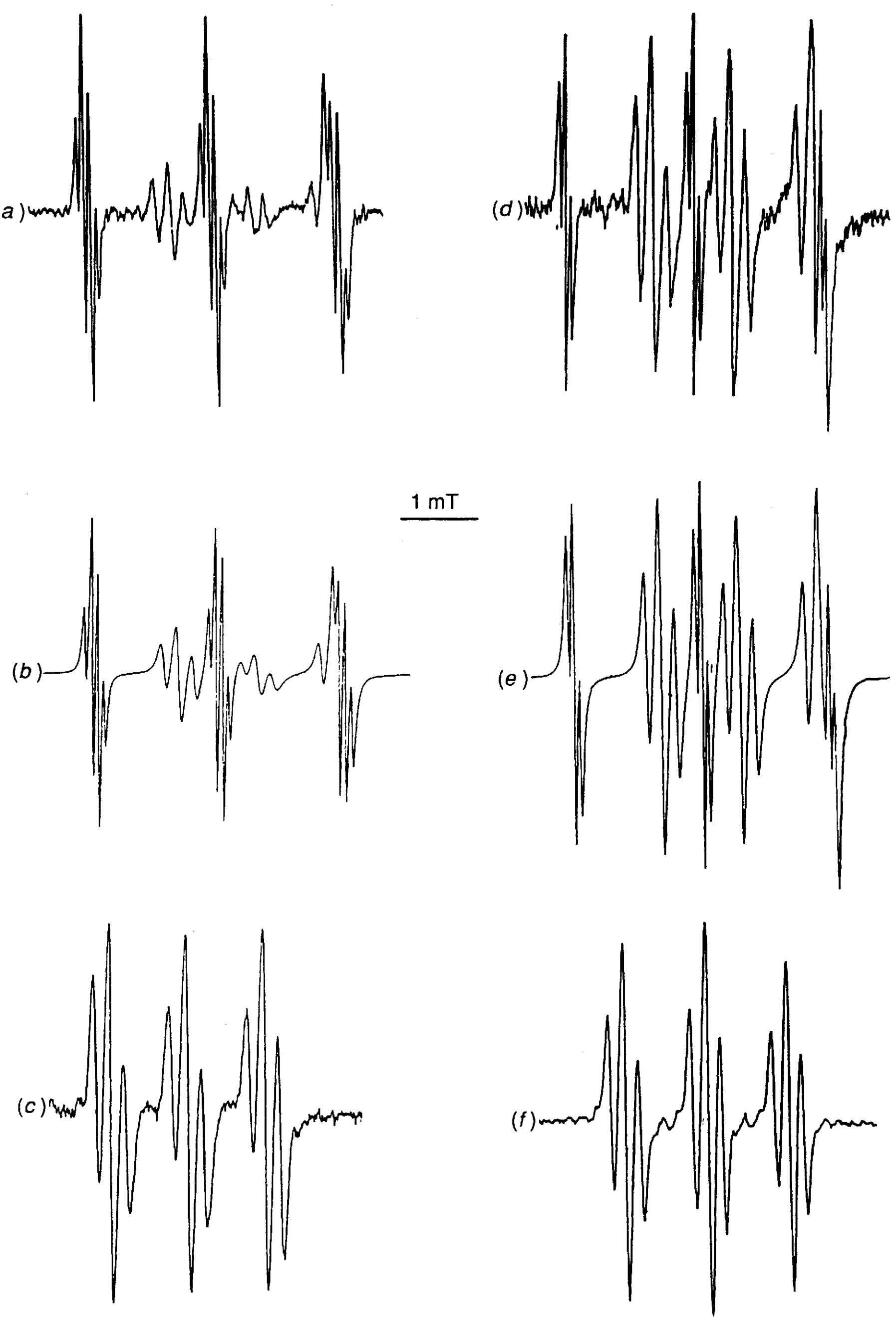

Fig. 3 Experimental and simulated EPR spectra of thiyl spin adducts of BNB in toluene. Adducts of (*a*) $Pr^iS^•$ (10^{-4} mol dm^{-3}), (*c*) $Pr^iS^•$ (neat disulfide), (*d*) $Bu^tS^•$ (10^{-4} mol dm^{-3}), (*f*) $Bu^tS^•$ (neat disulfide). (*b*) and (*e*) are simulations of spectra (*a*) and (*d*) using the parameters given in Table 2.

Changes in the Site of Addition with Disulfide Concentration.— On photolysis of isopropyl and *tert*-butyl disulfide, radicals were produced which added to both the nitrogen and oxygen positions of BNB. The thiyl oxygen adducts have similar coupling constants to the adducts from alkyl radicals, $Bu^{n•}$ and $(CH_3)_2CH^•$ [8] but the latter can be excluded because the additional 0.18 mT interaction with the isopropyl proton was absent from our spectra. It is also unlikely that the alkyl oxygen spin adducts are being observed since $(CH_3)_2CH^•$ would also be expected to add to the nitrogen of BNB to give a characteristic spectrum. In addition, we would expect that alkyl radicals would also be formed from other disulfides giving rise to spin adducts. Thus, the most likely explanation is that the more sterically hindered thiyl radicals are adding to both oxygen and nitrogen. This agrees with previous work [8] where it was found that the more sterically hindered the radical, the more likely it was to add to the oxygen. However, this does not explain the unexpected observation that addition to oxygen increases with an increase in the concentration of disulfide. We propose the following mechanism involving an RS–RSSR complex (Scheme 3) which reacts preferentially at oxygen to give the oxygen adduct releasing RSSR into solution. The complex, C, proposed here is similar to that suggested by Gilbert *et al.*[14] and Bonifačić *et al.*[15] for the reaction of $Bu^tO^•$ and $RS^•$ with disulfides.

When [NA] and [OA] have attained a steady state eqns. (1) and (2) apply.

$$\frac{d[NA]}{dt} = k_N[ST][RS^•] - k_{TN}[NA]_{SS} = 0 \qquad (1)$$

$$\frac{d[OA]}{dt} = k_O[ST][RS^•] + k_C[ST][C^•] - k_{TO}[OA]_{SS} = 0 \qquad (2)$$

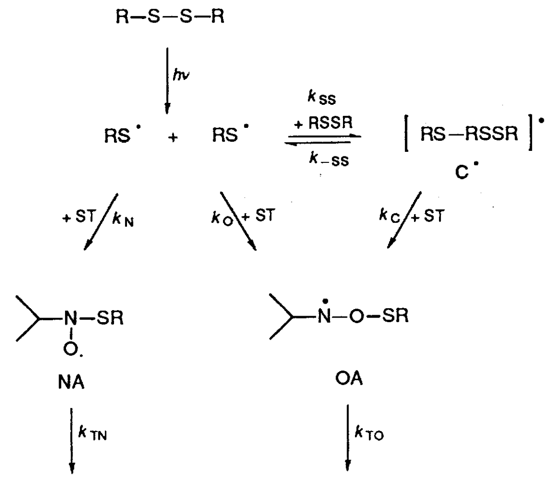

Scheme 3

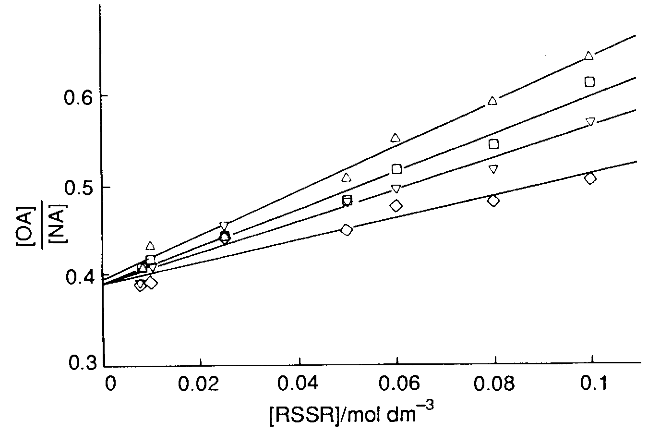

Fig. 4 A plot of $[OA]_{SS}/[NA]_{SS}$ at various spin trap concentrations against $[(Pr^iS)_2]$. $[ST] = 10^{-2}$ (◇), 5×10^{-3} (▽), 3.6×10^{-3} (□) and 2.5×10^{-3} (△) mol dm^{-3}.

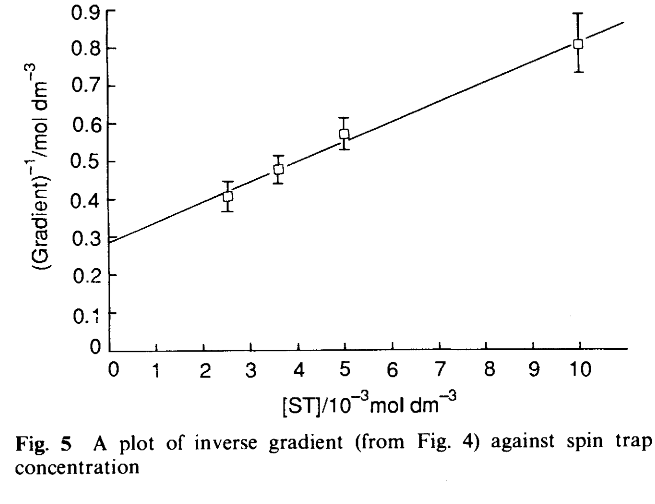

Fig. 5 A plot of inverse gradient (from Fig. 4) against spin trap concentration

Table 3 Ratios of rate constants obtained from Figs. 4 and 5 and from the decay of the spin adducts

Ratio	
k_{TN}/k_{TO}	4.5 ± 0.5
k_O/k_N	0.09 ± 0.01
k_N/k_{SS}	240 ± 36
k_{-SS}/k_C	$(5.6 \pm 2) \times 10^{-3}$ mol dm^{-3}

Thus, eqn. (3) may be derived.

$$\frac{[OA]_{SS}}{[NA]_{SS}} = \left(\frac{k_O}{k_N} + \frac{k_C[C^\bullet]}{k_N[RS^\bullet]}\right)\left(\frac{k_{TN}}{k_{TO}}\right) \quad (3)$$

Experimentally, the decays of both nitrogen and oxygen spin adducts were found to obey a first-order rate law in spin adduct concentration and k_{TN}/k_{TO} was estimated to be 4.5 ± 0.5. A similar first-order decay law was reported by Terabe *et al.*[16] for the thiyl adduct of nitrosodurene. However, second-order decays have also been reported for other nitroso adducts.[17,18]

Applying the steady state approximation to $[RS^\bullet]$ and $[C^\bullet]$ gives eqns. (4) and (5).

$$\frac{d[RS^\bullet]}{dt} = \Phi I - k_N[RS^\bullet][ST] - k_O[RS^\bullet][ST] - k_{SS}[RS^\bullet][RSSR] + k_{-SS}[C^\bullet] = 0 \quad (4)$$

$$\frac{d[C^\bullet]}{dt} = k_{ss}[RSSR][RS^\bullet] - k_{-SS}[C^\bullet] - k_C[C^\bullet][ST] = 0 \quad (5)$$

Transformation of eqn. (5) leads to eqn. (6) and substituting eqn. (6) into eqn. (3) gives eqn. (7).

$$\frac{[C^\bullet]}{[RS^\bullet]} = \frac{k_{SS}[RSSR]}{k_C[ST] + k_{-SS}} \quad (6)$$

$$\frac{[OA]_{SS}}{[NA]_{SS}} = \left(\frac{k_O}{k_N} + \frac{k_C k_{SS}[RSSR]}{k_N(k_C[ST] + k_{-SS})}\right)\frac{k_{TN}}{k_{TO}} \quad (7)$$

The predictions of eqn. (7) were tested by photolysing solutions of various concentrations of isopropyl disulfide and BNB and measuring the steady state concentrations of oxygen and nitrogen adducts. As shown in Fig. 4, at constant BNB concentration, the ratio $[OA]_{SS}/[NA]_{SS}$ increased linearly with disulfide concentration in accord with eqn. (7). Also the ratio increased with decreasing concentration of BNB again as predicted by eqn. (7). A constant intercept is also predicted in agreement with the experimental results.

From eqn. (7) a plot of the inverse gradient (from Fig. 4) against spin trap concentration should be linear with a gradient and intercept of:

$$\text{gradient} = \left(\frac{k_N}{k_{SS}}\right)\left(\frac{k_{TO}}{k_{TN}}\right)$$

$$\text{intercept} = \left(\frac{k_N}{k_C}\frac{k_{-SS}}{k_{SS}}\right)\left(\frac{k_{TO}}{k_{TN}}\right)$$

Fig. 5 shows that such a linear relationship is indeed found experimentally.

From Figs. 4 and 5 the ratios k_O/k_N, k_N/k_{SS} and k_{-SS}/k_C can be evaluated since k_{TN}/k_{TO} has been measured independently. The values obtained at 20 °C are listed in Table 3. They show that the rate constant for addition of $Pr^iS^\bullet$ radical to the nitrogen of BNB is about ten times higher than that for addition to the oxygen. The rate constant for the formation of the [RS–RSSR] complex is about 250 times lower than that for the reaction of $Pr^iS^\bullet$ with BNB. Ito and Matsuda[18] showed that nitroso compounds trap thiyl radicals with a rate constant of 10^8 dm^3 mol^{-1} s^{-1}. However, the nitroso compounds investigated were not as sterically hindered as BNB, thus a lower value of the rate constant would be expected for BNB. If the rate constant for direct formation of the spin adduct is assumed to be 10^7–10^8

$dm^3\ mol^{-1}\ s^{-1}$, then that for the formation of the complex is 10^5–10^6 $dm^3\ mol^{-1}\ s^{-1}$, indicating a fairly fast rate process with a collision efficiency of 10^{-4}–10^{-3} for this reaction in agreement with Bonifačič *et al.*[15] It is also worth noting that the ratio k_{-SS}/k_C of 5.5×10^{-3} means that it is not a good approximation to assume an equilibrium between $RS^\cdot$ and the complex at the concentration of BNB used here (0.01–0.0024 mol dm^{-3}), since the rate of the reverse reaction is comparable to that of the reaction of the complex with the spin trap ($k_{-SS}/k_C[ST] \equiv 0.05$–$2$).

Conclusions

(i) Both DMPO and BNB spin traps give thiyl adducts which allow an unequivocal determination of whether the thiyl carries a primary, secondary or tertiary alkyl or aryl group.

(ii) DMPO is an efficient trap for all thiyls whilst BNB is less efficient and does not trap aryl thiyls.

(iii) Radical addition of secondary and tertiary thiyls occurs at both nitrogen and oxygen centres with BNB and the oxygen addition increases with increasing concentration of disulfide. This is interpreted in terms of a thiyl–disulfide complex which effects addition exclusively at the oxygen centre. Rate constant data on the formation and reactions of this complex have been determined.

References

1 L. S. Harman, C. Mottley and R. P. Mason, *J. Biol. Chem.*, 1984, **259**, 5606; D. Ross, K. Norback and P. Maldew, *J. Biol. Chem.*, 1985, **260**, 5028.

2 J. R. Shelton and E. R. Harrington, *Rubber Chem. Technol.*, 1974, **49**, 147; W. J. M. Van Tilberg and P. Smael, *Rec. Trav. Chim.*, 1976, **95**, 132; A. J. Bridgewater and M. D. Sexton, *J. Chem. Soc., Perkin Trans. 2*, 1978, 530.

3 M. C. R. Symons, *J. Am. Chem. Soc.*, 1964, **91**, 5924.

4 E. G. Janzen, in *Free Radicals in Biology*, Ed. W. A. Pryor, Academic Press, New York, 1980, vol. 5, p. 115.

5 K. Saymol and A. R. Knight, *Can. J. Chem.*, 1968, **46**, 999.

6 G. H. Morine and R. R. Jantz, *Photochem. Photobiol.*, 1981, **33**, 1.

7 M. J. Davies, L. G. Forni and S. L. Shuker, *Chem. Biol. Interactions*, 1987, **61**, 177.

8 S. Terabe and R. Konaka, *J. Chem. Soc., Perkin Trans. 2*, 1973, 369.

9 P. D. Josephy, D. Rehorek and E. G. Janzen, *Tetrahedron Lett.*, 1984, **25**, 1685.

10 E. G. Janzen, C. A. Evans and J. I. Ping Liu, *J. Magn. Reson.*, 1973, **9**, 513.

11 E. G. Janzen and J. I. Ping-Liu, *J. Magn. Reson.*, 1973, **9**, 510.

12 O. Augusto, K. L. Kunze and P. R. Ortizole de Montellano, *J. Biol. Chem.*, 1982, **257**, 6231.

13 O. Ito and M. Matsuda, *Bull. Chem. Soc. Jpn.*, 1984, **57**, 1745.

14 B. C. Gilbert, C. M. Kirk, R. O. C. Norman and H. A. H. Lane, *J. Chem. Soc., Perkin Trans. 2*, 1977, 497.

15 M. Bonifačič and K.-D. Asmus, *J. Phys. Chem.*, 1984, **88**, 6286.

16 S. Terabe, K. Kurama and R. Konaka, *J. Chem. Soc., Perkin Trans. 2*, 1973, 1252.

17 T. Grillan and K. U. Ingold, *J. Am. Chem. Soc.*, 1971, **93**, 6555.

18 I. Osamu and M. Katsuda, *J. Am. Chem. Soc.*, 1983, **105**, 1937.

Paper 2/01824A
Received 30*th March* 1992
Accepted 26*th May* 1992